

# Chapter 16: Functional Measurements in Nuclear Medicine

Set of 71 slides based on the chapter authored by M.J. Myers

of the IAEA publication (ISBN 92-0-107304-6):

*Nuclear Medicine Physics:*

*A Handbook for Teachers and Students*

**Objective: To familiarize with functional measurements in diagnostic nuclear medicine**

Slide set prepared in 2015  
by M. Ferrari (IEO European  
Institute of Oncology,  
Milano, Italy)

## 16.1. INTRODUCTION

## 16.2. NON-IMAGING MEASUREMENTS

16.2.1. Renal function measurements

16.2.2. Carbon-14 breath tests

## 16.3. IMAGING MEASUREMENTS

16.3.1 Thyroid

16.3.2 Renal function

16.3.3 Lung function

16.3.4 Gastric function

16.3.5 Cardiac function

# 16.1 INTRODUCTION

The nuclear medicine modality focuses on **physiological organ function** for diagnoses.

The **three aspects** involved in the process are:

- I. **choice of radioactive tracer**
- II. **method of detection of the emissions from the tracer**
- III. **analysis of results of the detection.**

Different **methods of detection** can be used:

- Imaging with a gamma camera or PET scanner in a number of modes: **static**, **dynamic**, **whole body** and **tomographic**
- Counting over areas of the body which can also be static or dynamic
- Laboratory analysis of blood samples

## 16.2 NON IMAGING MEASUREMENTS

**Non-imaging measurements** refer to the analysis of data from radionuclide procedures that are not derived from interpreting normal and pathological patterns of uptake of tracer in images from  $\gamma$ -cameras and PET scanners.

**Example:** investigation of glomerular filtration in the kidney using a tracer such as  $^{51}\text{Cr}$ -EDTA which can be **measured from timed blood samples** without using images for information about morphological changes.

# 16.2 NON IMAGING MEASUREMENTS

## 16.2.1 Renal function measurements

Renal haemodynamic functions can be divided into measurements of :

- **renal blood flow:** supply of blood to the cortical and extramedullary nephrons which are the functional unit of the kidney
- **glomerular filtration:** transfer of fluids across the glomerulus

Several radioactive tracers may be used depending on the function to be studied, the most common being:

- ▶  $^{99m}\text{Tc}$  labelled diethylenetriaminepentaacetic acid (**DTPA**)
- ▶  $^{99m}\text{Tc}$  labelled dimercaptosuccinic acid (**DMSA**)
- ▶  $^{99m}\text{Tc}$  labelled mercaptoacetyltriglycine (**MAG3**)

## 16.2.1 Renal function measurements

### 16.2.1.1 *Glomerular filtration rate plasma clearance*

Calculation of **glomerular filtration rate (GFR)** is used in the general assessment of **renal function and the monitoring of renal function.**

Radioisotope measurements depend on the assessment of **plasma clearance** with time as seen with blood sampling of a tracer that is handled exclusively by glomerular filtration and does not enter blood cells. The most common radiopharmaceutical used is  $^{51}\text{Cr-EDTA}$ , though  $^{99\text{m}}\text{Tc-DTPA}$  and  $^{125}\text{I-iodothalamate}$  are also seen.

GFR is obtained by constructing the clearance curve from one or a series of timed measurements of plasma activity. In the multi-sample method, the expected multi-exponential curve is defined accurately with samples taken at 10, 20 and 30 min, and 2, 3 and 4 h, or approximated with samples taken at about 2 and 4 h.

## 16.2.1 Renal function measurements

### 16.2.1.1 Glomerular filtration rate plasma clearance

The object of the measurements is to construct **the total area under the plasma clearance curve**. It is sufficient for accuracy to assume a **bi-exponential curve** with a fast and slow component between times of 10 min and 4 h, *ignoring any initial very fast components*.

The zero time intercepts and rate constants for the fast and slow components are  $C_{10}$  and  $\alpha$ , and  $C_{20}$  and  $\beta$ , respectively.

$$\text{GFR} = \frac{\text{injected activity}}{\text{total area under plasma curve}} = \frac{Q_0}{A} = \frac{Q_0}{\frac{C_{10}}{\alpha} + \frac{C_{20}}{\beta}}$$

Where:  $Q_0$  [MBq]  
 $C_{10}$  and  $C_{20}$  [MBq/ml]  
 $\alpha$  and  $\beta$  [ $\text{min}^{-1}$ ]

GFR will vary with body size and is conventionally normalized to a standard body surface area of  $1.73 \text{ m}^2$ .

## 16.2.1 Renal function measurements

### 16.2.1.1 *Glomerular filtration rate plasma clearance*

As the contribution to the whole area from the fast component is relatively small and can be approximated without too much loss of accuracy, the **equation can be simplified to**

This produces an estimate of GFR that is obviously too small, though **with poor renal function the approximation has less of an effect.** A **correction factor** to convert the approximate GFR to the 'true' GFR can be used. Although this correction factor depends on the renal function, a figure of **1.15** can be used in most cases.

$$GFR = \frac{Q_0}{C_{20} / \beta}$$

The calculation for **GFR requires measurement** of the activity injected into the patient as well as the activity in the post-injection syringe, in a standard and in the blood samples. The counts recorded by the well counter measuring the small activities in the blood samples also have to be calibrated in terms of megabecquerels per count rate (MBq/count rate)

## 16.2.1 Renal function measurements

### 16.2.1.2 *Effective renal plasma flow measurements*

**Renal plasma flow**, also known as renal blood flow, has been investigated in the past using  $^{131}\text{I}$  or  $^{123}\text{I}$  labelled ortho-iodohippurate (hippuran) or para-amino hippurate (PAH).

Hippuran is almost completely excreted by the renal tubules and extracted on its first pass through the renal capillary system. As the extraction is not quite 100%, the renal function measured is called the **effective renal plasma flow (ERPF)**. A modern variation is to use the  $^{99\text{m}}\text{Tc}$  labelled tubular agent MAG3. However, the extraction fraction of MAG3 at below 50% is inferior to that of hippuran, so the **measurements of ERPF are simply estimates.**

**For the ERPF measurement a known activity of the radiopharmaceutical is injected and blood samples are taken at intervals, as for GFR.**

The timing of the intervals occurs at 5 min intervals and then at 30, 50, 70 and 90 min. The resulting two-exponential time–activity curve is plotted from which the function is given as:

$$ERFP = \frac{Q_0}{\frac{C_{10}}{\alpha} + \frac{C_{20}}{\beta}}$$

## 16.2 NON IMAGING MEASUREMENTS

### 16.2.2 Carbon-14 breath tests

The  $^{14}\text{C}$  urea breath test is used for detecting *Helicobacter pylori* infection

The test is based on the finding that the bacterium *H. pylori* produces the enzyme urease in the stomach. As urease is not normally found in that organ, its occurrence can, therefore, denote the existence of *H. pylori* infection.

The activity of  $^{14}\text{C}$  used in the test is very small (~ 37 kBq), and the effective dose < 3 mSv

# 16.2 NON IMAGING MEASUREMENTS

## 16.2.2 Carbon-14 breath tests

<sup>14</sup>C urea is administered orally in the form of a **capsule**.

The urease in the stomach converts the urea to ammonia and <sup>14</sup>C carbon dioxide which is exhaled and **can be detected in breath samples using a liquid scintillation counter**.

The counter can measure minute quantities of the beta emitting <sup>14</sup>C. One or two samples are usually collected after 10–30 min using a straw and balloon technique. Also counted are a known standard sample and a representative background sample.

The net disintegrations per minute (dpm) registered by the counter are compared with standard values to assess the degree of infection. DPM is given by:

$$\text{dpm} = \frac{(S - B) \times S_t}{(S_t - B)}$$

where

$S$  is sample counts per minute;  
 $B$  is blank counts per minute;  
 $S_t$  is standard counts per minute.

## 16.3 IMAGING MEASUREMENTS

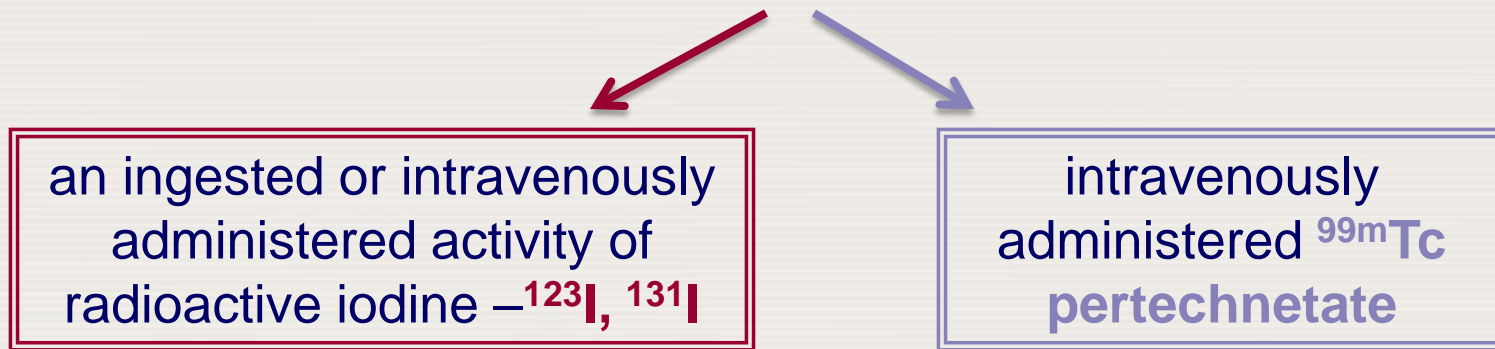
**Imaging measurements** include

- **static image** acquisition and analysis for quantitative assessment of uptake, example: thyroid uptake measurement
- **time–activity curves derived from dynamic 2-D imaging** and quantitative parameters assessed from images, example: renal function
- **time–activity curves derived from dynamic 3-D imaging** with quantitative parameters assessed from physiologically triggered images, example: cardiac ejection fraction measurement.

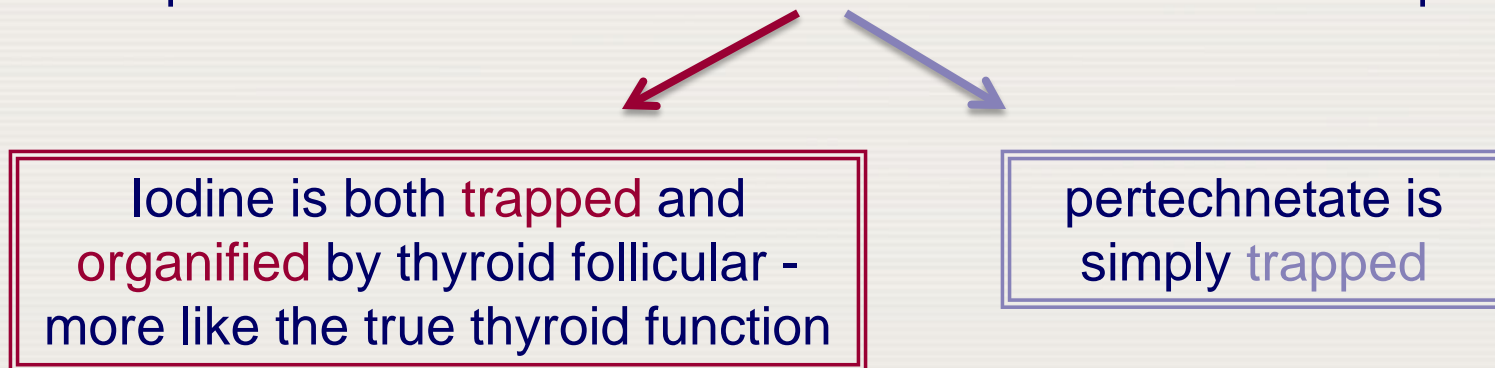
# 16.3 IMAGING MEASUREMENTS

## 16.3.1 Thyroid

**Tests on the thyroid** consist of **both imaging the morphology** of the organ and **assessing its 'uptake'**. Uptake consists of measuring the activity taken up by the gland of:



The uptake mechanisms are different for the two radioisotopes



# 16.3 IMAGING MEASUREMENTS

## 16.3.1 Thyroid

The tests allow assessment of:

- **functionality of thyroid lesions and nodules**, and investigations of **thyroiditis** and **ectopic tissue**. They can confirm a diagnosis of an **excess of circulating thyroid hormones**, (Graves' disease and toxic nodular goitre), and lead to a more **quantitative approach to treatment of hyperthyroidism with  $^{131}\text{I}$**
- **uptake of tumours secondary to thyroid cancer** that have disseminated through the body following surgery may also be assessed. In this case, whole body images are made using  $^{131}\text{I}$  and a scanning gamma camera. The tumours can be located and, in some cases, a quantitative measurement of uptake made, thus allowing the effectiveness of treatment to be monitored

# 16.3 IMAGING MEASUREMENTS

## 16.3.1 Thyroid

The **choice of radiopharmaceutical** used can be dictated by the **availability** and **cost** of the preferred isotope  $^{123}\text{I}$  and  $^{99\text{m}}\text{Tc}$ . Each is suitable for use with a  $\gamma$ -camera.

$^{123}\text{I}$

- half-life: 13 h
- gamma emission: 160 keV
- cyclotron produced is not readily available and is expensive

$^{99\text{m}}\text{Tc}$

- half-life: 6 h
- gamma emission: 140 keV
- readily available from the standard hospital molybdenum generator

The timing of the uptake of the two isotopes is also different

$^{123}\text{I}$  18–24 h after injection  
2–6 h after ingestion

$^{99\text{m}}\text{Tc}$  20 min after injection

# 16.3 IMAGING MEASUREMENTS

## 16.3.1 Thyroid

**Uptake measurement with a scintillation probe** involves counting over

- the neck
- a 'thyroid phantom'
- over the thigh of the patient to simulate background counts

The **thyroid phantom** consists of a small source of known activity in a plastic cylinder offering the same attenuation as a neck. This acts as the standard.

Counts are obtained at a distance of about 25 cm from the collimator face to offset any inverse square errors due to different locations of the thyroid.



## 16.3 IMAGING MEASUREMENTS

### 16.3.1 Thyroid

The **percentage uptake**  $U$  is then calculated from the formula:

$$U = \frac{N - T}{C_a} \times 100$$

where

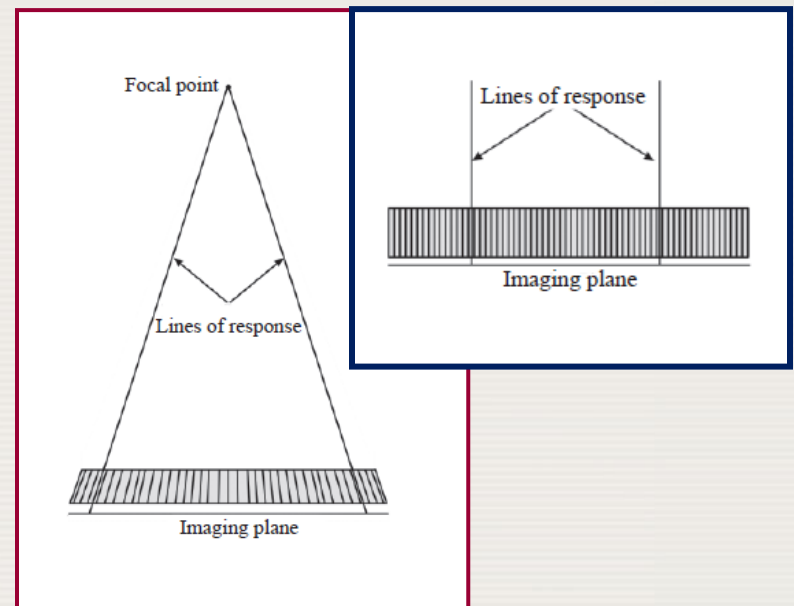
- $N$  is the counts in the neck;
- $T$  is the counts in the thigh;
- $C_a$  is the administered counts corrected for background (measured directly with an isotope calibrator before the test or can be related to the activity in the thyroid phantom). Corrections for decay are made throughout.

# 16.3 IMAGING MEASUREMENTS

## 16.3.1 Thyroid

Similar measurements can be made with the **gamma camera** in place of the probe, except that corrections for neck uptake can be made **using ROIs** over the delineated thyroid and regions away from the gland.

The camera can be fitted with a **pinhole collimator** in order to provide a degree of magnification, although the image is somewhat distorted. Images obtained with a **parallel hole collimator** may appear smaller but are not prone to distance effects, though subject to the same attenuation.



**Anterior views** are generally enough but a **lateral view** may also be used to locate ectopic tissue.

# 16.3 IMAGING MEASUREMENTS

## 16.3.1 Thyroid

Quantification of the uptake is achieved in two ways:

- by **calibrating the camera** with a known activity in a suitable phantom, the activity injected into the patient can be measured
- by **measuring the injection** directly in the syringe before administration.

Each will yield the **sensitivity of the camera** in terms of **counts/MBq** and allow the activities seen in the thyroid glands and background to be calculated.

The process is often an automatic one performed by the camera computer software that delineates the outlines of the thyroid lobe(s) and establishes a suitable background region used to correct for the presence of activity in tissue overlying and underlying the thyroid underlying tissue correction.

It is important that a local **normal range** is established and that the calibration of the camera in terms of counts per megabecquerel is subject to a **quality assurance programme**.



# 16.3 IMAGING MEASUREMENTS

## 16.3.2 Renal function *16.3.2.1 General discussion*

The study of **renal function** has been a mainstay of nuclear medicine for many decades and is an established efficient technique for, among other functions, assessing **renal perfusion**, **quantifying divided or individual kidney function**, and **studying output efficiency and obstruction**.

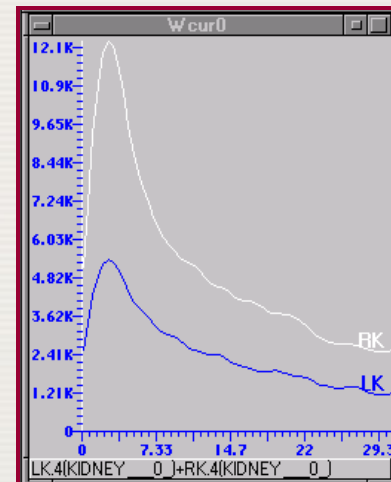
**Two aspects** of renal function are exploited:

- **glomerular filtration**, i.e. the transfer of fluids across the glomerulus, investigated by measuring the clearance of  **$^{99m}\text{Tc-DTPA}$**  (*pentetate*);
- **tubular secretion**, investigated by measuring the clearance of  **$^{99m}\text{Tc-MAG3}$**  (*tiatide*)

# 16.3 IMAGING MEASUREMENTS

## 16.3.2 Renal function *16.3.2.2 Renal function measurements*

The bases of measurements of most renal functions are **time–activity curves** obtained by imaging the kidneys using a  $\gamma$ - camera. Views are obtained at different times and over different periods after administration of one of a number of radiotracers and often after some intervention. The result is usually a curve, called a 'renogram', showing the rise and fall of counts in each kidney.



## 16.3 IMAGING MEASUREMENTS

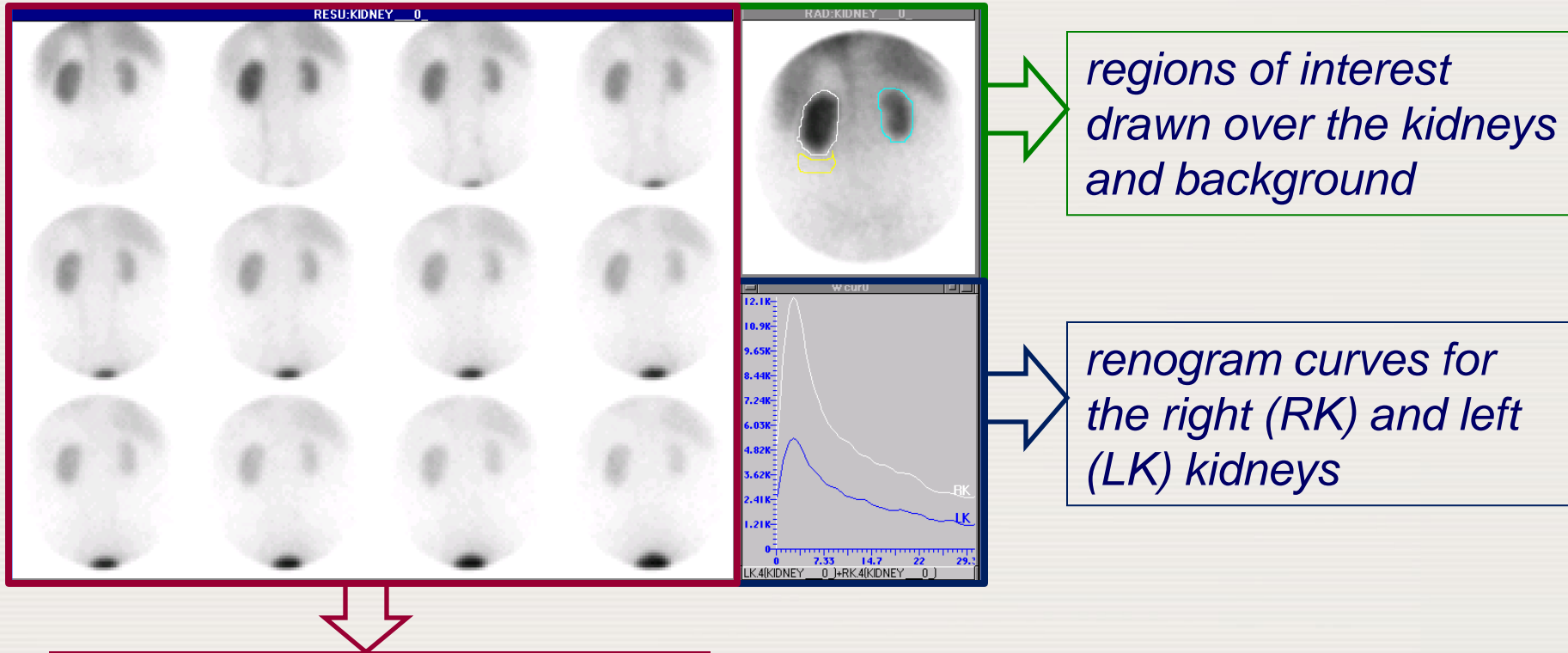
### 16.3.2 Renal function *16.3.2.2 Renal function measurements*

The analysis programmes, supported by **commercial software providers**, allow the calculation of a number of **renal function parameters**, including relative perfusion, relative function, mean and minimum transit times, and outflow efficiency.



# 16.3 IMAGING MEASUREMENTS

## 16.3.2 Renal function *16.3.2.2 Renal function measurements*



*Dynamic renal flow study after administration of  $^{99m}\text{Tc-MAG3}$*

## 16.3 IMAGING MEASUREMENTS

### 16.3.2 Renal function *16.3.2.2 Renal function measurements*

*What is happening to the tracer as it traverses the kidneys, and how it appears in the images and renogram?*

After adjustment for the contributions of activity in the renal vasculature, the corrected curve displaying a relatively fast rise and subsequent slower fall in activity can be described by **two distinct phases**:

- the first spans the time of injection to the end of the minimum transit time when the kidney contains the sum of all of the tracer extracted from the blood and has, therefore, been termed the **sum phase**
- the second starts at the end of the first and reflects the net activity left after loss from the kidney and has been called the **difference phase**

## 16.3 IMAGING MEASUREMENTS

### 16.3.2 Renal function *16.3.2.2 Renal function measurements*

- What is helpful is often a **quantitative comparison of the two kidneys with derivation of a relative function**. This may be calculated from **Patlak plots** or from the **uptake slope** or the integral of the renogram curves.
- The programme can calculate the relative perfusion and function from the retention functions.
- In the case of assessment of **kidney transplants**, other aspects can be used to calculate relevant parameters.

# 16.3 IMAGING MEASUREMENTS

## 16.3.3 Lung function

The functions of the lung that are investigated using nuclear medicine techniques are:

- regional ventilation
- pulmonary blood flow or perfusion (ventilation perfusion ratio)
- intrapulmonary vascular shunting
- pulmonary granulocyte kinetics
- lung tissue permeability.

Lung air flow or ventilation imaging is carried out either with a gas such as:

- $^{81\text{m}}\text{Kr}$  (a 13 s half-life radioisotope generated from  $^{81}\text{Rb}$  that has a 4.6 h half-life)
- an aerosol containing particles of sizes between 0.1 and 2  $\mu\text{m}$ , typically  $^{99\text{m}}\text{Tc}$ -DTPA or carbon particles (*Technegas*)

# 16.3 IMAGING MEASUREMENTS

## 16.3.3 Lung function

- **Lung blood flow or perfusion** imaging is carried out with macroaggregates or microspheres of denatured human serum albumin (**MAA**).
- These particles of average size 20–40  $\mu\text{m}$  are larger than the lung capillaries and are **trapped in the capillary bed**, distributing according to the blood flow to a region.
- Their main use is to **image pulmonary vascular disease** (pulmonary embolism)
- The **two techniques are often employed together**, either **simultaneously** (e.g.  $^{81}\text{Kr}$  and  $^{99\text{m}}\text{Tc}$  MAA) or **sequentially** ( $^{99\text{m}}\text{Tc}$  aerosol and  $^{99\text{m}}\text{Tc}$  MAA).
- The **presence or absence of ventilation and/or perfusion** is of **clinical** significance.

## 16.3 IMAGING MEASUREMENTS

### 16.3.4 Gastric function

Nuclear medicine allows a full, non-invasive and quantitative assessment of the way the **oesophagus moves both solid and liquid meals to the stomach**, how the stomach handles these meals and how they transit through the gastrointestinal tract.

## 16.3 IMAGING MEASUREMENTS

### 16.3.4 Gastric function *16.3.4.1 Stomach emptying of solid and liquid meals*

As the choice of both solid and liquid test meals determines the **standard values** used as criteria for evaluating the function, **a 'standard meal' has been agreed**. Solid meals are based on preparations including eggs (into which  $^{99m}\text{Tc}$  sulphur colloid has been mixed), toast and water.

Anterior and posterior dynamic images are obtained at suitable intervals of time following ingestion of the meal and are repeated for the same positioning at hourly intervals for up to 4 h.

## 16.3 IMAGING MEASUREMENTS

### 16.3.4 Gastric function *16.3.4.1 Stomach emptying of solid and liquid meals*

- The reason for the two view approach is to obtain a geometric mean of the activity in the field of view that accounts for the movement of activity between the anterior and posterior surfaces of the body. Relying on a simple anterior view leads to artefacts due to differential attenuation of the  $^{99m}\text{Tc}$  gamma rays.
- The data is analysed by **drawing ROIs** around the organs of interest (stomach and parts of the gastrointestinal tract) and creating a **decay corrected time–activity curve**. An assessment of the gastric emptying function is made from standard values. An alternative way of expressing the result is through the half-emptying time.

## 16.3 IMAGING MEASUREMENTS

### 16.3.4 Gastric function *16.3.4.2 Analysis of colonic transit*

**Colonic transport analysis** can be performed using  $^{111}\text{In}$  labelled non-absorbable material, such as DTPA or polystyrene micropellets administered orally. Indium-111 is chosen because of its longer half-life (2.7 d) and the possibility of imaging over a longer time since images are taken at, for example, 6, 24, 48 and 72 h.

## 16.3 IMAGING MEASUREMENTS

### 16.3.4 Gastric function *16.3.4.2 Analysis of colonic transit*

- The **geometric mean** parametric image of anterior and posterior views may be used in the quantification.
- A **geometric centre of the activity** (also called centre of mass) may be tracked over time by defining particular segments in the colon, perhaps 5–11 in number (e.g. the ascending, transverse, descending, rectosigmoid and excreted stool), multiplying the individual segment counts by weighting factors from 1 to 5 respectively, and summing the resulting numbers.

## 16.3 IMAGING MEASUREMENTS

### 16.3.4 Gastric function *16.3.4.2 Analysis of colonic transit*

In addition to **time–activity curves** for the individual **segments**, the rate of movement of the geometric centre as a function of time can be assessed by plotting this as a time position profile. A colonic half-clearance time may be calculated and compared with historical normal control values of colonic transport.

## 16.3 IMAGING MEASUREMENTS

### 16.3.4 Gastric function *16.3.4.3 Oesophageal transit*

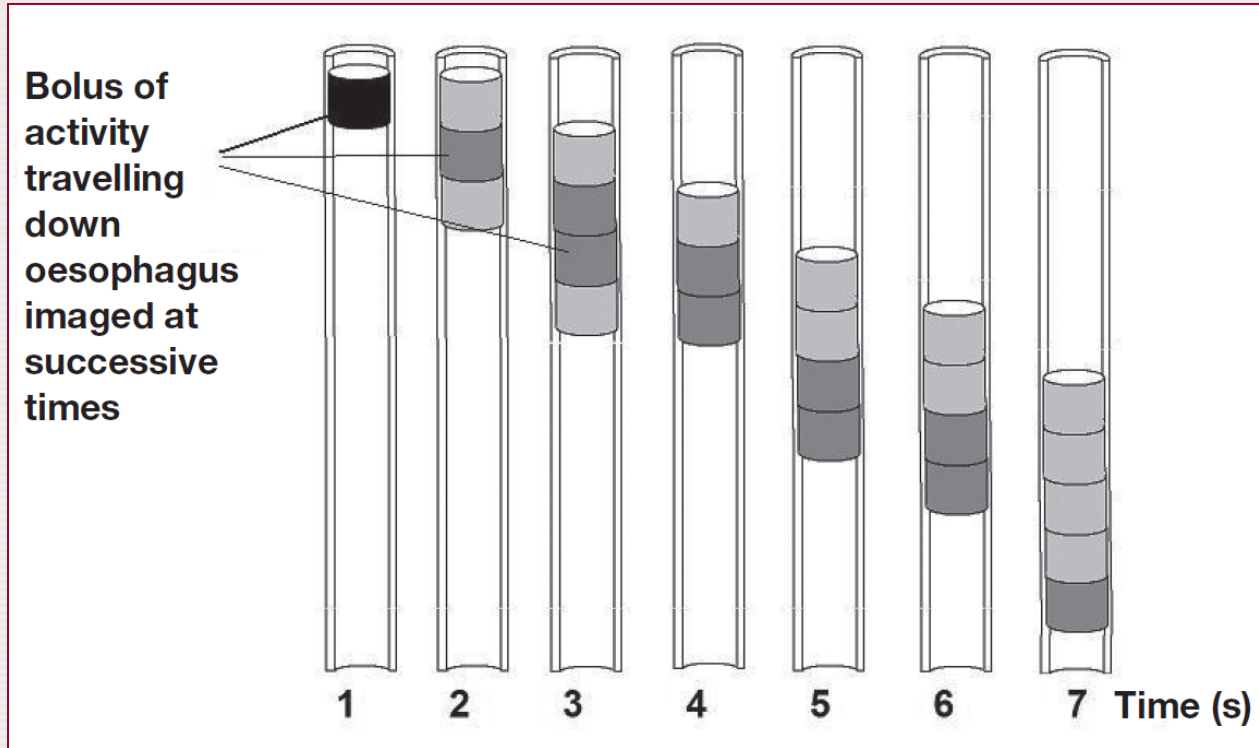
The **oesophageal transit** is studied by imaging the **transit of a bolus of radiolabelled non-metabolized material** such as  $^{99m}\text{Tc}$  sulphur colloid.

Either the whole oesophagus may be included in an ROI and a time–activity curve generated for the whole organ, or a special display may be generated, whereby the counts in successive regions of the oesophagus are displayed on a 2-D space–time map called a condensed image.

The counts in the regions are displayed in the y direction as colour or grey scale intensities corresponding to the count rate against time along the x axis. The result is a **pictorial idea of the movement of the bolus down the oesophagus.**

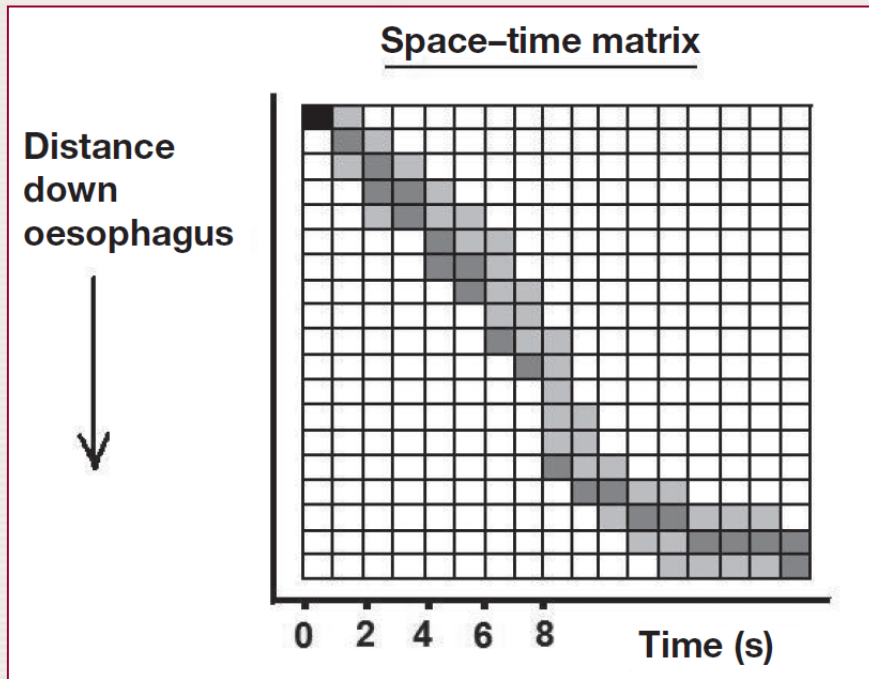
# 16.3 IMAGING MEASUREMENTS

## 16.3.4 Gastric function *16.3.4.3 Oesophageal transit*



## 16.3 IMAGING MEASUREMENTS

### 16.3.4 Gastric function *16.3.4.3 Oesophageal transit*



**Oesophageal transit is imaged as a space-time matrix.** As the bolus of radioactivity passes down the oesophagus, the counts from successive regions of interest, represented on a grey scale, are placed in consecutive positions in the matrix in the appropriate time slot.

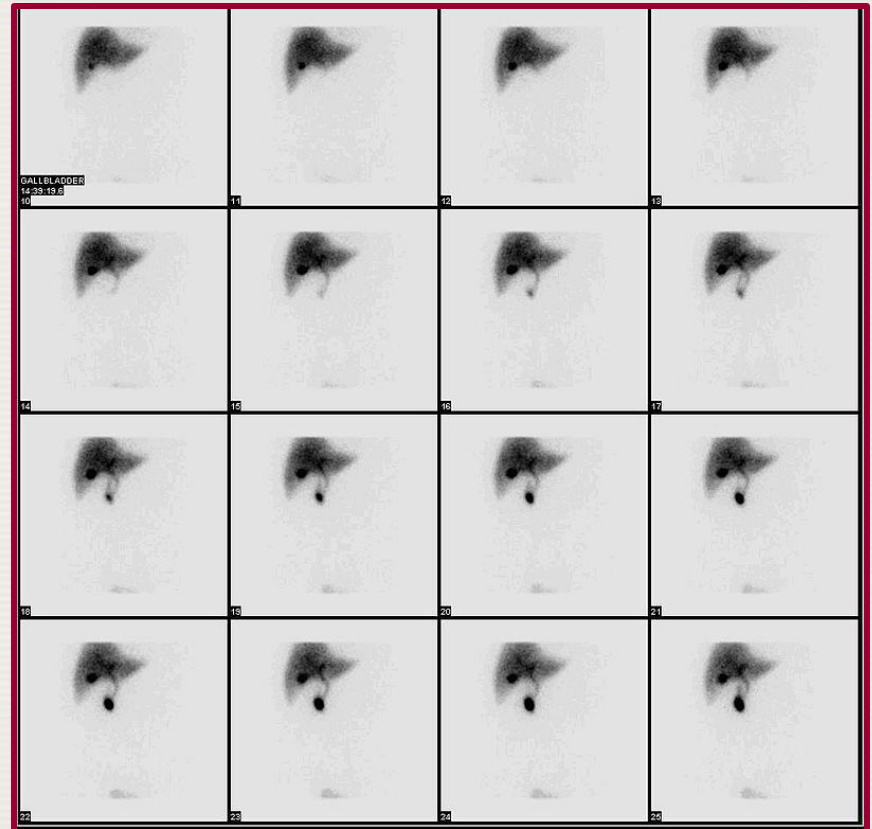
A **normal transit** will be shown as a movement of the **bolus down and to the right in the matrix**. **Retrograde peristalsis** will be shown as a **movement to the right and upwards**.

## 16.3 IMAGING MEASUREMENTS

### 16.3.4 Gastric function *16.3.4.4 Gall bladder ejection function*

The **gall bladder** is investigated using **hydroxy iminodiacetic acid labelled with  $^{99m}\text{Tc}$** .

This is injected and can be imaged using a gamma camera after excretion by the liver into the bile and as it passes through the gall bladder and bile ducts. The gall bladder is then made to contract and empty by injecting a hormone called **cholecystikinin** and the imaging of the gall bladder continued, the whole test taking between 1 and 2 h.



## 16.3 IMAGING MEASUREMENTS

### 16.3.4 Gastric function *16.3.4.4 Gall bladder ejection function*

The amount of the radiolabel that leaves the gall bladder is assessed by the difference in counts in the ROI over the emptied gall bladder divided by the counts from the ROI over the full gall bladder. Expressed as a percentage, this gives **the ejection fraction**. An ejection fraction **above 50%** is considered as normal and an ejection fraction **below about 35%** as abnormal, suggesting, for example, chronic acalculous cholecystitis.

# 16.3 IMAGING MEASUREMENTS

## 16.3.5 Cardiac function

- The two main classes of cardiac function are **blood flow in the myocardium and in the blood pool** and **ventricles**.
- Images are acquired in both **planar and tomographic modes**, and the data may be acquired **dynamically** over sequential time periods or as a **gated study triggered by the electrocardiogram (ECG)**, or as part of a **first-pass study**.
- The information is presented on a global or regional basis as **conventional or parametric images**, or as curves from which quantitative parameters may be derived.
- A **range of pharmaceutical agents** labelled with single and positron emitting isotopes are used.

# 16.3 IMAGING MEASUREMENTS

## 16.3.5 Cardiac function

**Cardiac functions** that may be investigated:

- myocardial perfusion
- myocardial metabolism of glucose and fatty acids
- myocardial receptors
- left ventricular ejection fraction
- first-pass shunt analysis
- wall motion and thickness
- stroke volumes
- cardiac output and its fractionation
- circulation times
- systolic emptying rate
- diastolic filling rate
- time to peak filling or emptying rate
- regional oxygen utilization

## 16.3 IMAGING MEASUREMENTS

### 16.3.5 Cardiac function

**Commercial suite of programmes** will usually only offer a **limited selection of functional analysis**. Typically, these include blood pool gated planar or SPECT analysis for ventricular volumes and ejection fractions, and cardiac perfusion analysis of gated SPECT images acquired under stress/rest conditions.



## 16.3 IMAGING MEASUREMENTS

### 16.3.5 Cardiac function

In addition to the aspect of the software provided is the **choice of radiopharmaceutical available**. A wide choice is theoretically possible, depending on the particular function to be explored.

For example:

myocardial receptors



$^{123}\text{I}$ -MIBG (metaiodobenzylguanidine)  
or  $^{11}\text{C}$ -hydroxyephedrine

myocardial glucose



$^{18}\text{F}$ -FDG (fluorodeoxyglucose)

fatty acid metabolism



$^{123}\text{I}$ -heptadecanoic acid or  
BMIPP ( $\beta$ -methyl-p-iodophenylpentadecanoic acid)

## 16.3 IMAGING MEASUREMENTS

### 16.3.5 Cardiac function

**SPECT techniques** use  $^{201}\text{Tl}$ ,  $^{99\text{m}}\text{Tc}$ -sestamibi and other perfusion agents.

**PET** viability studies can employ  $^{13}\text{N}$ -ammonia,  $^{18}\text{F}$ -FDG and  $^{11}\text{C}$ -acetate.

## 16.3 IMAGING MEASUREMENTS

### 16.3.5 Cardiac function *16.3.5.2 First-pass angiography*

**First-pass studies** typically involve the acquisition of about 2000 frames of data at a duration of ~ 50 ms following the **bolus injection of autologous red blood cells labelled** in vivo or in vitro **with  $^{99m}\text{Tc}$**  as they pass through the right ventricle for the first time. A **time–activity curve** derived from an **ROI over the ventricle** shows a curve that rises to a peak and then falls off, the curve also showing a saw tooth pattern **corresponding to the filling and emptying of the left ventricle during the cardiac cycle.**

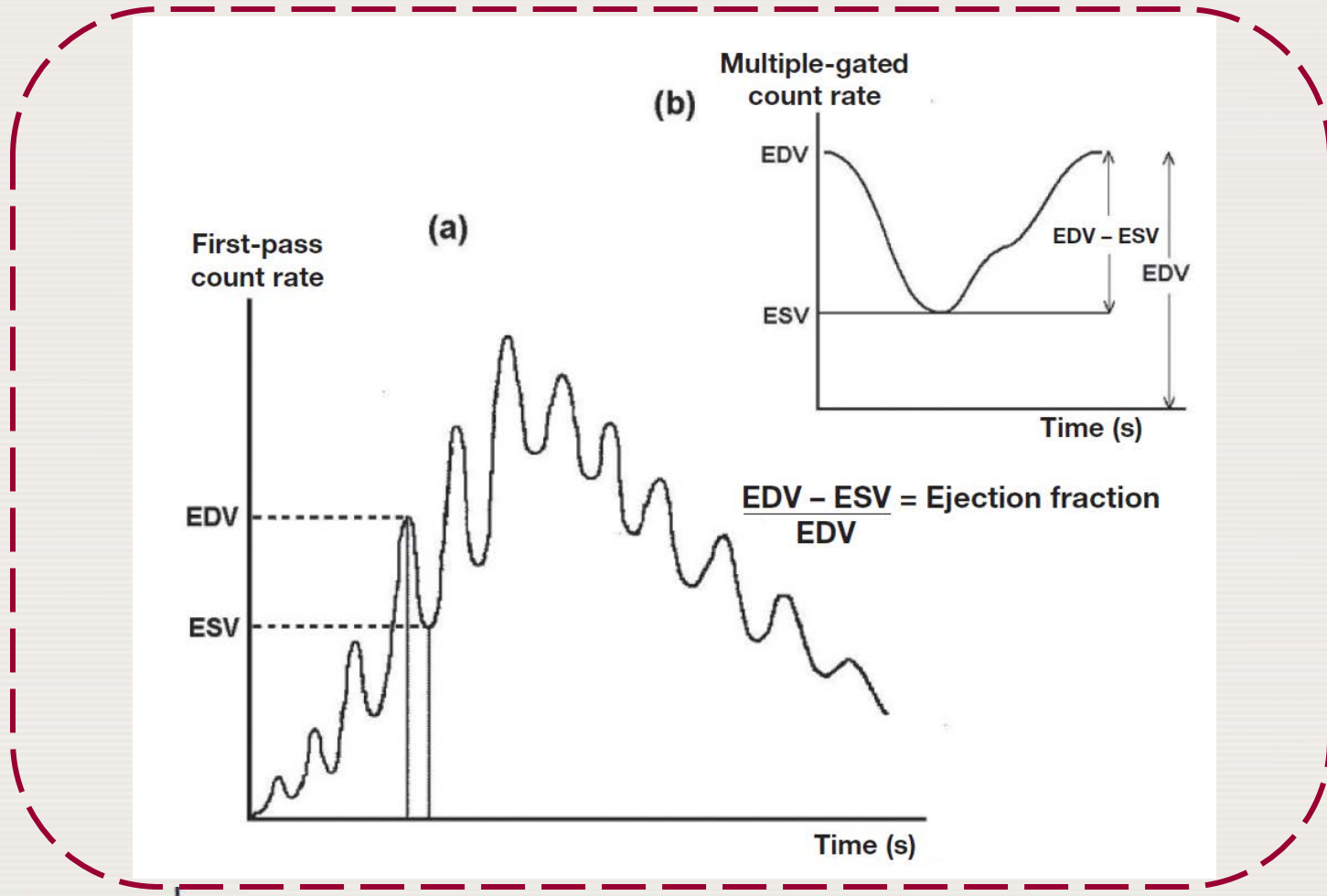
## 16.3 IMAGING MEASUREMENTS

### 16.3.5 Cardiac function *16.3.5.2 First-pass angiography*

- By suitable **positioning of the gamma camera in the right anterior oblique view**, this saw tooth can be used as an estimate of ejection fraction in the right ventricle, a parameter that is only amenable to analysis in the first pass before uptake in adjoining structures.
- The **ejection fraction** is derived from the ratio of the peak of any saw tooth (**the end diastolic volume (EDV)**) minus the value of the next trough (**the end systolic volume (ESV)**) to the EDV. The ejection fraction for the left ventricle would be assessed from the curve obtained by viewing in the left anterior oblique position.

# 16.3 IMAGING MEASUREMENTS

## 16.3.5 Cardiac function *16.3.5.2 First-pass angiography*



## 16.3 IMAGING MEASUREMENTS

### 16.3.5 Cardiac function *16.3.5.2 First-pass angiography*

- Although this parameter is **more reliably obtained from a MUGA** study, the **first-pass procedure is much quicker** and may be suitable for patients who cannot tolerate the much longer MUGA study.
- First-pass kinetics also provide a measure of left to right cardiac shunts and the pulmonary systemic flow ratio, as well as systolic emptying and diastolic filling rates and ventricular volumes.

## 16.3 IMAGING MEASUREMENTS

### 16.3.5 Cardiac function *16.3.5.3 The multiple-gated acquisition scan MUGA*

- The **MUGA scan** traces heart muscle activity from the distribution of the administered radiopharmaceutical, allowing the calculation of the **left ventricular ejection fraction and demonstrating myocardial wall motion**.
- It may be obtained while the patient is at **rest** and after physically or pharmacologically induced **stress**.
- **Autologous red blood cells** labelled in vivo or in vitro with  $^{99m}\text{Tc}$  are injected as a **bolus**.
- The  $\gamma$ -camera views the patient in the left anterior oblique position so as to best **separate the projections of the two ventricles**.

## 16.3 IMAGING MEASUREMENTS

### 16.3.5 Cardiac function 16.3.5.3 The multiple-gated acquisition scan MUGA

**Dynamic images of the left ventricle in a beating heart are acquired** at the same time as the ECG and the results stored. A trigger (*gating signal*) corresponding to the R wave marks the start of each heart cycle and the start of each sequence of images. The time period between successive R waves (*R–R interval*) is divided into time intervals and the beat by beat left ventricular images corresponding to each time interval are each integrated into a single combined ‘gated’ image that **provides a stop motion image of the heart at intervals in its cycle.**

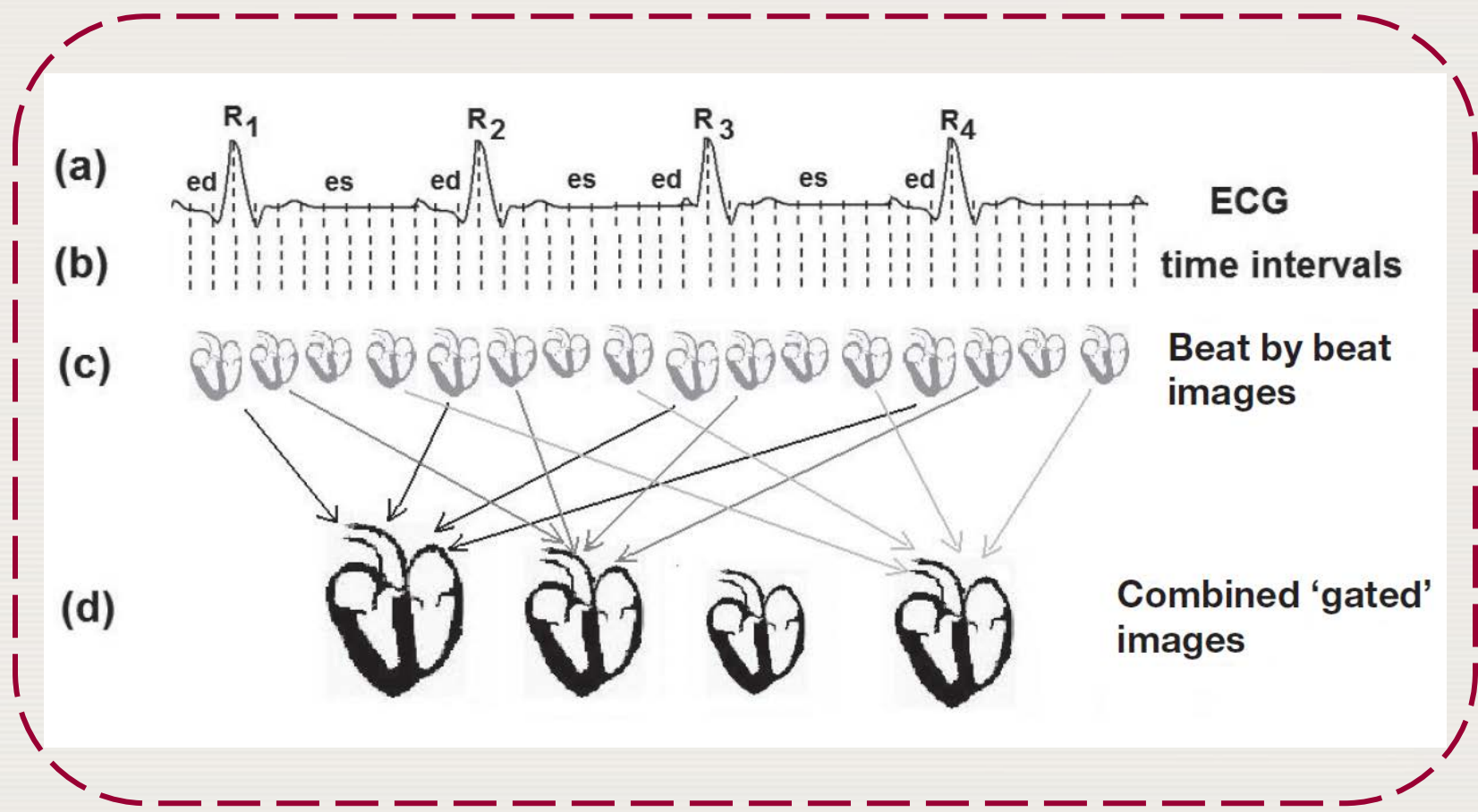
## 16.3 IMAGING MEASUREMENTS

### 16.3.5 Cardiac function 16.3.5.3 *The multiple-gated acquisition scan MUGA*

- As any one frame would not have enough data to provide sufficient counts and would, therefore, be statistically unreliable, **many frames at the same interval are superimposed on each other.**
- The signal for the start of each sequence is derived from an **ECG monitor** connected to the patient that provides a short electronic pulse as it detects the peak of an R wave. Usually, about 32 equally time-spaced frames (*multiple gates*) are used and these are defined between each R–R interval. **Beats within 10% of the mean length are accepted.**
- The result is a **series of images of the heart at end diastole and at end systole**, and at stages in between.

# 16.3 IMAGING MEASUREMENTS

## 16.3.5 Cardiac function *16.3.5.3 The multiple-gated acquisition scan MUGA*



## 16.3 IMAGING MEASUREMENTS

### 16.3.5 Cardiac function *16.3.5.3 The multiple-gated acquisition scan MUGA*

- The **image at end diastole when the heart has filled with blood contains the maximum number of counts**, and the end systolic image the least number.
- A direct **relationship** is made between the number of counts in a **region of the ventricle and its volume**.
- For each frame, the computer, starting with an initial rough outline provided by the operator, **defines the boundary of the left ventricle**.

## 16.3 IMAGING MEASUREMENTS

### 16.3.5 Cardiac function *16.3.5.3 The multiple-gated acquisition scan MUGA*

Depending on the computer programme used, a different method of edge detection may be employed:

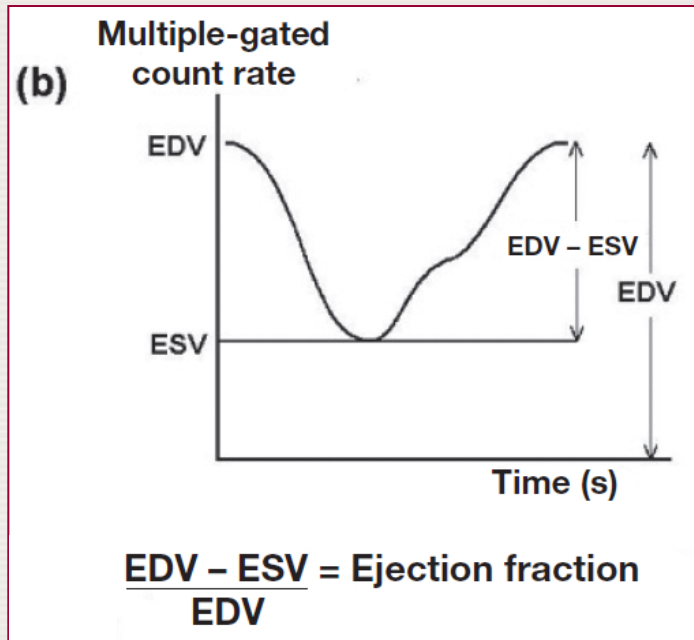
- isocount contour
- maximum slope normal to the edge.

As there is interference with the ventricular image from activity seen in pulmonary blood, the computer will also define a **suitable background ROI** close to the wall and correct the ventricular image at each stage.

## 16.3 IMAGING MEASUREMENTS

### 16.3.5 Cardiac function 16.3.5.3 The multiple-gated acquisition scan MUGA

The plot of the counts in the ventricular region vs. time forms the volume curve that starts with the EDV, falls to the ESV level and rises again.



Simple differentiation of the volume curve provides **indices of the ventricular filling and emptying rates**. Indeed, if the cardiac output is known, the rates can be **quantified** in terms of **millilitres per minute**.

## 16.3 IMAGING MEASUREMENTS

### 16.3.5 Cardiac function *16.3.5.4 Myocardial perfusion imaging*

**Myocardial perfusion imaging** allows a regional assessment of blood flow to the heart and demonstrates areas of **ischaemic myocardium** where the blood flow is diminished when the patient undergoes a **stress test**.

Imaging follows administration of specific radiopharmaceuticals such as  **$^{201}\text{Tl}$ -chloride**,  **$^{99\text{m}}\text{Tc}$ -tetrofosmin** or  **$^{99\text{m}}\text{Tc}$ -sestamibi** after the patient has been subjected to **physical exercise** or, if this is not suitable, to **pharmacological stress** with vasodilators to raise the heart rate and stimulate the myocardium.



## 16.3 IMAGING MEASUREMENTS

### 16.3.5 Cardiac function *16.3.5.4 Myocardial perfusion imaging*

It is also possible to use  **$\beta^+$  emitting radiopharmaceuticals** such as

- **$^{13}\text{N}$ -ammonia** (10 min half-life, produced by cyclotron)
- **$^{82}\text{Rb}$**  (75 s half-life, produced by generator).

## 16.3 IMAGING MEASUREMENTS

### 16.3.5 Cardiac function *16.3.5.4 Myocardial perfusion imaging*

- **Once a stable ECG pattern** is observed, the patient is imaged using a  $\gamma$ -camera operating in **SPECT mode**
- ECG gating is applied throughout and **produces sets of 16 images at each acquisition angle**
- The **stress images** and their analysis may be **compared** with similar ones obtained with the **patient at rest**.
- **Different protocols** (times of examination, radiopharmaceutical) have been devised to carry out the stress/rest examinations in one/two days, given the potential long washout periods involved.

## 16.3 IMAGING MEASUREMENTS

### 16.3.5 Cardiac function *16.3.5.4 Myocardial perfusion imaging*

Imaging can be performed '**early**' (at ~ 15 min) following injection of  $^{201}\text{Tl}$  or  $^{99\text{m}}\text{Tc}$ -sestamibi at rest or after the stress test and/or '**delayed**' (after 1–4 h or after 24 h) after injection at rest or under stress of the longer lived  $^{201}\text{Tl}$ .

**These protocols give rise to different types of image.**

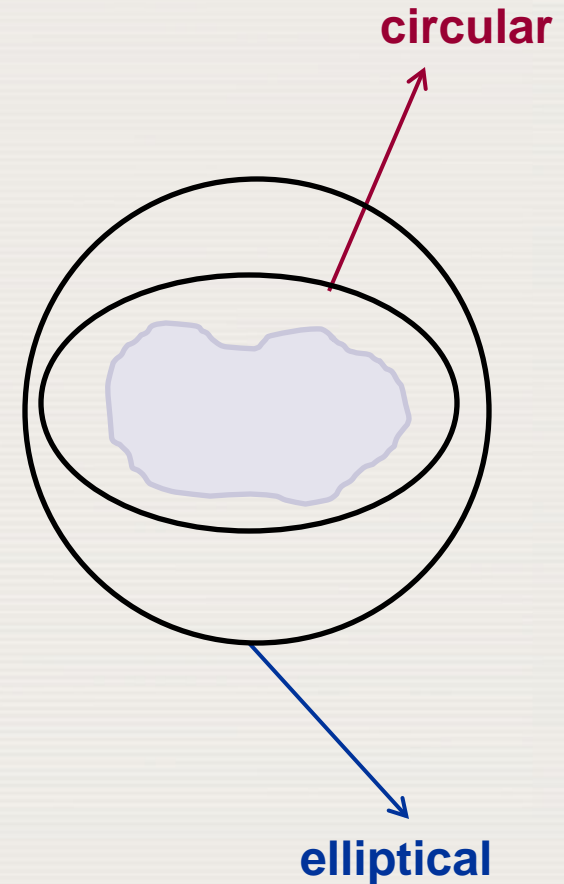
In general, the imaging properties of  $^{99\text{m}}\text{Tc}$  **give superior images**, though  $^{201}\text{Tl}$  **is superior from a physiological viewpoint** as it is a better potassium analogue.

# 16.3 IMAGING MEASUREMENTS

## 16.3.5 Cardiac function *16.3.5.4 Myocardial perfusion imaging*

Conventional cardiac SPECT imaging may be carried out with a **single or double headed gamma** camera using **circular or elliptical orbits**, the latter allowing closer passes over the patient and, consequently, better resolution.

Attenuation correction may be performed on the emission images using an isotope or CT X ray source.



## 16.3 IMAGING MEASUREMENTS

### 16.3.5 Cardiac function *16.3.5.5 Technical aspects of SPECT and PET*

There are different **sources of degradation** of the image quality in SPECT.

**Attenuation: Thallium** is not an ideal  $\gamma$  camera imaging radionuclide; it emits **low energy characteristic X rays** between 69 and 80 keV that are easily attenuated and, therefore, lost in the body.

The **attenuation varies for the different projections** around the body and **gives rise to artefacts** in the perfusion images if not corrected.

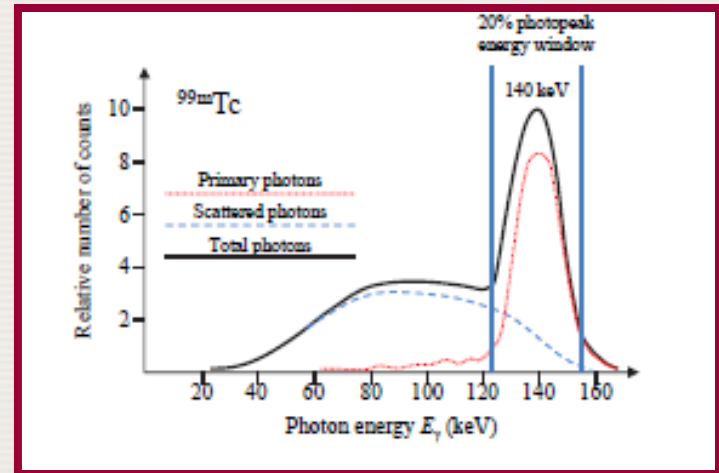
The 140 keV  $\gamma$  energy of  $^{99m}\text{Tc}$ , while still liable to attenuation, allows better collection of data from the heart and **less variation in the attenuation**.

**SPECT/CT** would be a **better option for attenuation correction** than the isotope attenuation correction devices that have been used in the past.

# 16.3 IMAGING MEASUREMENTS

## 16.3.5 Cardiac function *16.3.5.5 Technical aspects of SPECT and PET*

**Scatter:** Scattering of the  $\gamma$ -photons before detection in the camera leads to problems in that their origin might be misplaced and loss from deeper structures occurs. Recently, software to reduce the effects of scattering by modelling its behaviour within the field of view has become available.



## 16.3 IMAGING MEASUREMENTS

### 16.3.5 Cardiac function *16.3.5.5 Technical aspects of SPECT and PET*

**Resolution:** Another source of degradation of the image quality is the loss of resolution with distance from the collimator face.

Although 'high' resolution collimators are usually chosen for  $^{99m}\text{Tc}$  imaging, the basic resolution of the camera at the level of the heart is rather poor. Again, software techniques to model this behaviour and correct for it have become available.

## 16.3 IMAGING MEASUREMENTS

### 16.3.5 Cardiac function *16.3.5.5 Technical aspects of SPECT and PET*

**Statistic:**  $\gamma$ -camera images, are always subject to lack of counts and are, therefore, prone to statistical errors. Using a double headed rather than a single headed system is, therefore, an advantage. There is still discussion on the best angle between the heads and this may vary between less than  $90^\circ$  and  $180^\circ$ . Scanning the patient with the collimator as close to the source of activity as possible also ensures the best resolution, so a non-circular orbit is usually chosen. Owing to the lack of accessible counts with  $^{201}\text{Tl}$ , a general purpose collimator is used, which is more efficient but less accurate than the high resolution collimator used with  $^{99\text{m}}\text{Tc}$ .

## 16.3 IMAGING MEASUREMENTS

### 16.3.5 Cardiac function *16.3.5.5 Technical aspects of SPECT and PET*

**PET:** PET imaging is more sensitive and more accurate (better resolution) than SPECT and uptake of the radiopharmaceuticals can be quantified absolutely.

In theory, the use of  $^{13}\text{N}$  labelled ammonia and  $^{18}\text{F}$ -FDG can differentiate more about the state of the myocardium, its blood flow and metabolism, than the SPECT tracers.

## 16.3 IMAGING MEASUREMENTS

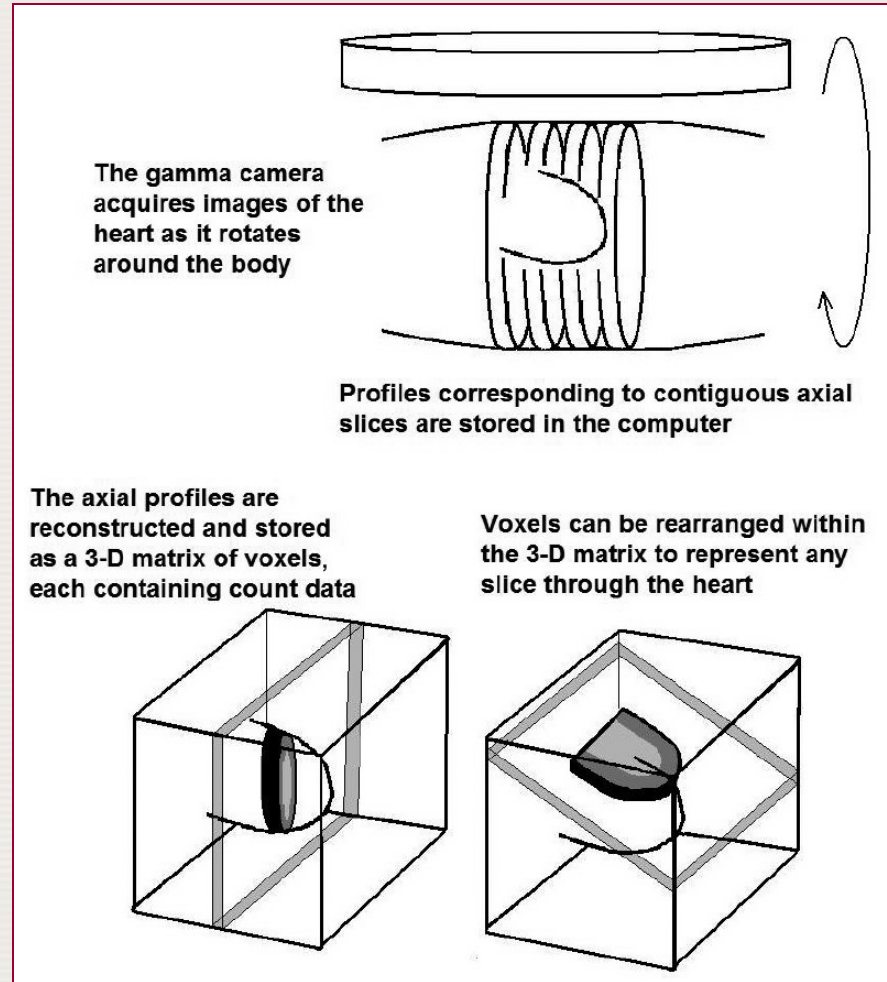
### 16.3.5 Cardiac function *16.3.5.5 Technical aspects of SPECT and PET*

**Reorientation:** As the heart lies at an angle to this body axis, a process of reorientation is performed. From the original matrix, the data that lay parallel to the axes of the heart itself can be selected to form vertical long axis (parallel to the long axis of the left ventricle and perpendicular to the septum), horizontal long axis (parallel to the long axis of the left ventricle and to the septum) and short axis (perpendicular to the long axis of the left ventricle) slices through the myocardium of the particular patient

# 16.3 IMAGING MEASUREMENTS

## 16.3.5 Cardiac function *16.3.5.5 Technical aspects of SPECT and PET*

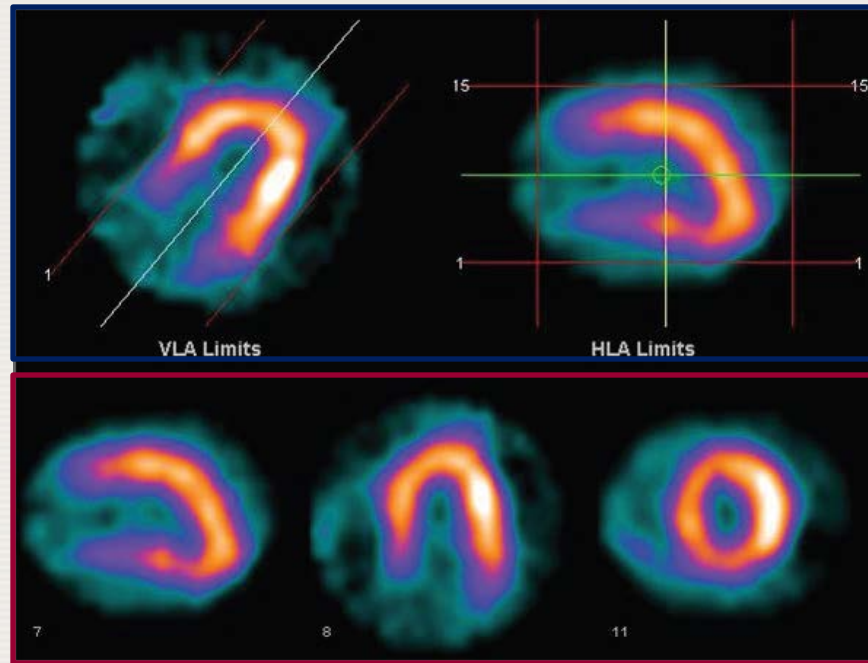
**Principle of rearrangement of acquired axial tomographic images into slices aligned with the axes of the heart:**



# 16.3 IMAGING MEASUREMENTS

## 16.3.5 Cardiac function 16.3.5.5 Technical aspects of SPECT and PET

*Orthogonal views of myocardial perfusion SPECT with orientation of the slices along the long axis of the heart*



*Original trans-axial slice through the myocardium with the white line indicating the long axis (left) and a sagittal slice (right)*

*the reoriented views with the vertical and horizontal slices through the long axis, and a slice perpendicular to the long axis (from left to right).*

## 16.3 IMAGING MEASUREMENTS

### 16.3.5 Cardiac function *16.3.5.5 Technical aspects of SPECT and PET*

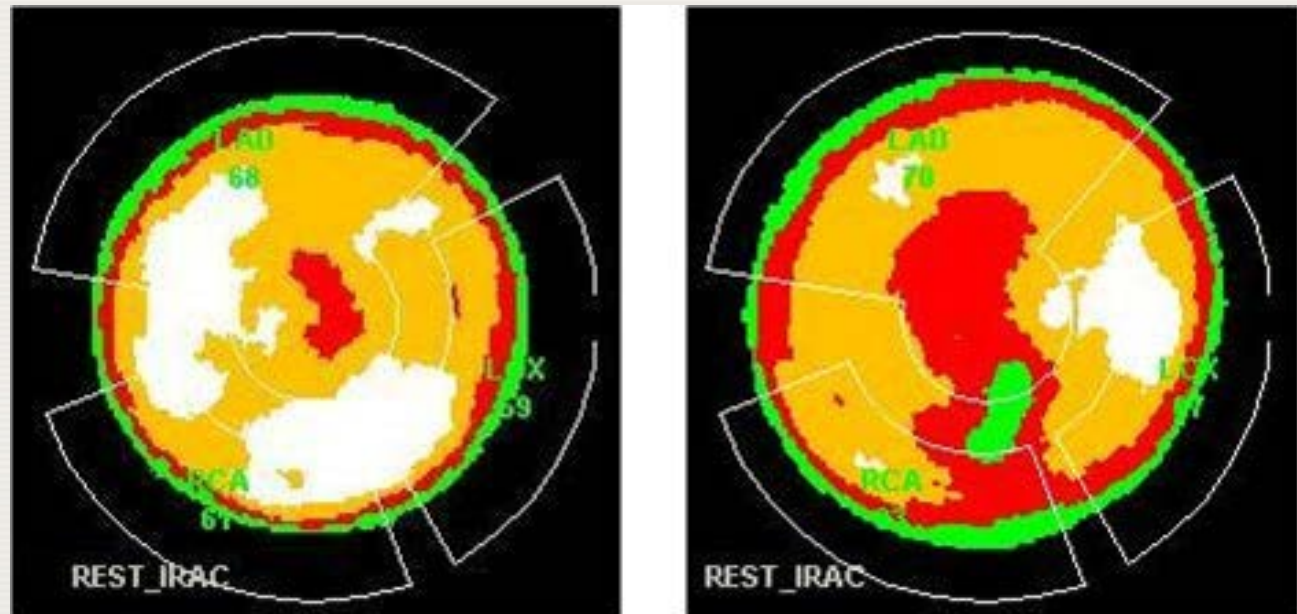
Cardiac processing software, working on features extracted from the shape of the myocardium, allows easy automatic alignment which may also be operator guided. The reoriented sections form three sets of images that are displayed in a standard format to show, for example, the apex and heart surfaces at each stage of gating of the heart cycle.

Presentation of the slice data is often as a so-called ***polar diagram or bull's-eye display***, this allows the 3-D information about the myocardium, which would be difficult to interpret easily, to be depicted as a simple, 2-D, colour coded, semi-quantitative image.

## 16.3 IMAGING MEASUREMENTS

### 16.3.5 Cardiac function *16.3.5.5 Technical aspects of SPECT and PET*

***Bull's-eye displays of myocardial SPECT perfusion studies.*** Normal perfusion (left) and hypo-perfusion of inferior wall (right). The colours indicate the degree of perfusion, with white — normal, orange — acceptable, red — hypo-perfused and green — no perfusion. Also indicated are the perfusion areas for the main coronary vessels LAD, LCX and RCA.



## 16.3 IMAGING MEASUREMENTS

### 16.3.5 Cardiac function *16.3.5.5 Technical aspects of SPECT and PET*

The process is often described as imagining the myocardial surface as the peel of half an orange which is flattened out to form the polar diagram. This is divided into accepted segments and values, and colours associated with each segment.

There is a **variation of the exact form and mathematical basis of the polar diagram in the commercial products available**. This results in different looking maps that, although individually validated, are **not directly comparable**.

It would, therefore, be prudent for one software package to be standardized at any one reporting centre. The results from a particular study can be compared with a reference image derived from a so-called normal database to allow a better estimation of the extent of the defects.

# CHAPTER 16 BIBLIOGRAPHY

- PETERS, A.M., MYERS, M.J., Physiological Measurements with Radionuclides in Clinical Practice, Oxford University Press, Oxford (1998).
- ZIESSMAN, H.A., O'MALLEY, J.P., THRALL, J.H., Nuclear Medicine— The Requisites, 3rd edn, Mosby-Elsevier (2006).

## FURTHER READING

Recommended methods for investigating many of these functions may be found on the web sites of the American Society of Nuclear Medicine ([www.snm.org](http://www.snm.org)), the British Nuclear Medicine Society ([www.bnms.org.uk](http://www.bnms.org.uk)) and the International Committee for Standardization in Haematology (<http://www.islh.org/web/published-standards.php>).

